Electroreduction of Oxygen in a Series of Room Temperature Ionic Liquids Composed of Group 15-Centered Cations and Anions

Russell G. Evans,[†] Oleksiy V. Klymenko,[†] Sahar A. Saddoughi,[†] Christopher Hardacre,[‡] and Richard G. Compton*,[†]

Physical and Theoretical Chemistry Laboratory, University of Oxford, South Parks Road, Oxford, OX1 3QZ, United Kingdom, and School of Chemistry, The Queen's University of Belfast, Belfast, Northern Ireland, BT9 5AG, United Kingdom

Received: December 11, 2003; In Final Form: March 18, 2004

The electrochemical reduction of oxygen is reported in four room temperature ionic liquids (RTILs) based on quaternary alkyl -onium cations and heavily fluorinated anions in which the central atom is either nitrogen or phosphorus. Data were collected using cyclic voltammetry and potential step chronoamperometry at gold, platinum, and glassy carbon disk electrodes of micrometer dimension under water-free conditions at a controlled temperature. Analysis via fitting to appropriate theoretical equations was then carried out to obtain kinetic and thermodynamic information pertaining to the electrochemical processes observed. In the quaternary ammonium electrolytes, reduction of oxygen was found to occur reversibly to give stable superoxide, in an analogous manner to that seen in conventional aprotic solvents such as dimethyl sufoxide and acetonitrile. The most significant difference is in the relative rate of diffusion; the diffusion coefficients of oxygen in the RTILs are an order of magnitude lower than in common organic solvents, and for superoxide these values are reduced by a further factor of 10. In the quaternary phosphonium ionic liquids, however, more complex voltammetry is observed, akin to that expected for the reduction of oxygen in acidified organic media. This is shown to be consistent with the occurrence of a proton abstraction reaction between the electrogenerated superoxide and quaternary alkyl phosphonium cations following the initial electron transfer.

Introduction

The electrochemistry of dioxygen has been thoroughly investigated in conventional aqueous and organic solvents, and is reviewed in a recent publication by Sawyer,[1] himself a significant contributor in this field. These studies have proven that reduction of the oxygen molecule is a complex process, the outcome of which is highly dependent on the solvent employed and, in particular, its acidity. In aprotic media (acetonitrile, dimethylformamide, dimethyl sulfoxide) a reversible, one-electron reduction occurs to yield the superoxide ion, $O_2^{-\bullet}$.[2−4]

$$O_2 + e^- \rightleftharpoons O_2^{-\bullet} \quad (1)$$

Regardless of solvent, this radical anion is highly reactive and behaves as a strong Brønsted base in the presence of a proton source. Accordingly, addition of a Brønsted acid to the aprotic solvent brings about a change in the observed voltammetry; the reversible one-electron signal is replaced by an irreversible two-electron wave as the electrogenerated superoxide rapidly undergoes a series of protonation and disproportionation steps to ultimately yield hydrogen peroxide as the final product.[2,5,6]

$$O_2 + 2e^- + 2H^+ \rightarrow H_2O_2 \quad (2)$$

Recently, room temperature ionic liquids (RTILs) have become popular alternative solvents in which to conduct electrochemical investigations (for a review see ref 7), and the reduction of oxygen in these media has already been the subject of several reports.[8−12] The first such study was performed by Carter et al. who reported the voltammetry of dioxygen at a 3 mm diameter glassy carbon (GC) electrode in the basic chloroaluminate binary molten salt 1-ethyl-3-methylimidazolium chloride/aluminum chloride.[8] A single cathodic peak was observed and interpreted in terms of reaction 2 above, that is, reduction to superoxide followed by fast irreversible reaction with protonic impurities present within the melt. Attempts to stabilize the superoxide by eliminating these protonic impurities proved unsuccessful. In a subsequent study, AlNashef and co-workers analyzed the reduction of oxygen at a GC macroelectrode in two RTILs consisting of the 1,2-dimethyl-3-*n*-butylimidazolium and 1-methyl-3-*n*-butylimidazolium cations, respectively, combined in each case with the hexafluorophosphate anion.[10] In the former ionic liquid, an ill-defined reduction wave with no reverse peak was observed and again attributed to the influence of impurities endemic to the RTIL. In the second ionic liquid, however, the electrogenerated superoxide was stable enough to be observed by cyclic voltammetry (reaction 1) and partake in follow-up reactions with gaseous carbon dioxide introduced to the RTIL, as explored in a subsequent report.[11] Most recently, our group has studied the reduction of oxygen in two ionic liquids, 1-ethyl-3-methylimidazolium bis(trifluoromethylsulfonyl)imide, [EMIM][$N(Tf)_2$], and *n*-hexyltriethylammonium bis(trifluoromethylsulfonyl)imide, [N_{6222}][$N(Tf)_2$], at a 10 μm diameter gold disk electrode.[12] In this investigation, stable superoxide was successfully generated in both liquids, and analysis of a combination of chronoamperometric measurements and cyclic voltammetry

* To whom correspondence should be addressed. Phone: 01865 275413. Fax: 01865 275410. E-mail: richard.compton@chemistry.ox.ac.uk.
[†] University of Oxford.
[‡] The Queen's University of Belfast.

10.1021/jp031309i CCC: $27.50
Published on Web 05/18/2004

CHART 1: Structures of the Ions Comprising the RTILs under Investigation

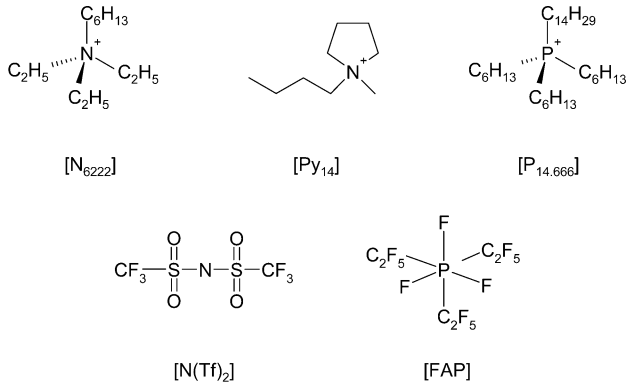

allowed the diffusion coefficients of both oxygen and superoxide to be determined in these media. The most interesting results were seen for the second ionic liquid, $[N_{6222}][N(Tf)_2]$, in which these diffusion coefficients were found to differ by more than a factor of 30, giving rise to a pronounced asymmetry in the forward and backward voltammetric waves; both transient and steady-state behavior was observed in a single voltammogram.

In light of these initial results, the aim of the present study was to carry out a comprehensive investigation of the electrogeneration of stable superoxide in various ionic liquid solvents and characterize the heterogeneous kinetics for this process at electrodes composed of different materials (gold, platinum, and GC). Four RTILs were employed, all consisting of complex ions based around central nitrogen and phosphorus atoms, namely, the following: $[N_{6222}][N(Tf)_2]$; *N*-methyl-*N*-butylpyrrolidinium bis(trifluoromethylsulfonyl)imide, $[Py_{14}][N(Tf)_2]$; tris(*n*-hexyl)tetradecylphosphonium bis(trifluoromethylsulfonyl)-imide, $[P_{14.666}][N(Tf)_2]$; and tris(*n*-hexyl)tetradecylphosphonium trifluorotris(pentafluoroethyl)phosphate, $[P_{14.666}][FAP]$ (for structures see Chart 1). The three cations involved are all long chain quaternary alkyl -onium ions, preferred over possible imidazolium-based alternatives due to the more favorable results they yielded in our preliminary study[12] and, since the reaction of interest is a reduction, the inherently larger cathodic potential windows these types of ionic liquids have been found to possess.[13−15] Early on, it was appreciated that strict control over the experimental temperature would be essential to allow the collection of reliable data. The viscosities of ionic liquids are extremely temperature dependent (a 20% change over 5 K not being uncommon[16]), and the effect of this is felt electrochemically primarily through the approximately inverse relationship between solution viscosity and rate of diffusion of dissolved species.[17] While this should be a concern in any study, in experiments involving gaseous substrates the effect of temperature variation is exacerbated by its potentially large effect on their solubility. Consequently, a temperature-controlled box was constructed to house the electrochemical cell and thus permit the measurement of reproducible results under well-defined conditions. With this in place, a series of voltammetric and chronoamperometric experiments were performed and the resulting data analyzed against the appropriate theories to produce a set of thermodynamic and kinetic parameters for the reduction of oxygen. These results are discussed and compared with the equivalent behavior reported for traditional aprotic solvents.

Experimental Section

Chemical Reagents. RTILs *n*-hexyltriethylammonium bis(trifluoromethylsulfonyl)imide, $[N_{6222}][N(Tf)_2]$, *N*-methyl-*N*-butylpyrrolidinium bis(trifluoromethylsulfonyl)imide, $[Py_{14}][N(Tf)_2]$, and tris(*n*-hexyl)tetradecylphosphonium bis(trifluoromethylsulfonyl)imide, $[P_{14.666}][N(Tf)_2]$, were prepared from the corresponding chloride salt using standard literature methods.[13,18] Tris(*n*-hexyl)tetradecylphosphonium trifluorotris(pentafluoroethyl)phosphate, $[P_{14.666}][FAP]$, was obtained from Merck KGaA (for structures see Chart 1). Pureshield argon, oxygen (both BOC, Surrey, UK), catechol (Aldrich, 99+%), ferrocene (Aldrich, 98%), tetrabutylammonium perchlorate (TBAP, Fluka, puriss electrochemical grade, >99%), and acetonitrile (Fisher Scientific, dried and distilled, >99.99%) were used without further purification.

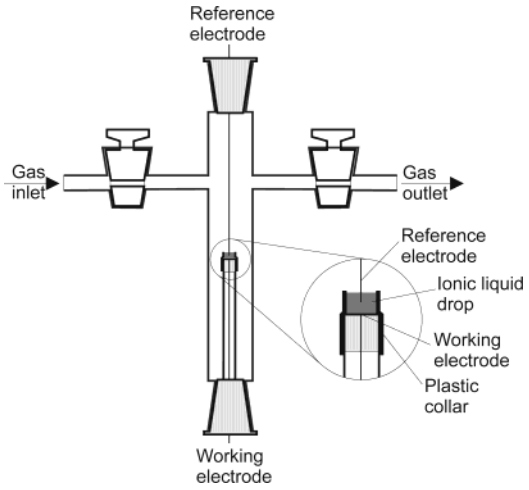

Figure 1. Cross section of the cell used to perform electrochemical experiments on microliter solutions of oxygen in RTILs under a controlled atmosphere.

Instrumentation. Electrochemical experiments were performed using a computer-controlled μ-Autolab (Eco-Chemie, Utrecht, Netherlands). A conventional two-electrode arrangement was employed with a 0.5 mm diameter silver wire (99.99%, Advent Research Materials Ltd., Oxfordshire, UK) acting as a quasi-reference electrode. The working electrodes used (Cypress Systems, Kansas) consisted of gold, platinum (both 10 μm nominal diameter), and glassy carbon (11 μm nominal diameter) wires sealed into glass capillaries, the ends of which were polished to expose a disk-shaped surface. These electrodes were polished prior to each experiment, first using a 1.0 μm alumina−water slurry (Buehler, Illinois) on a polishing pad (Kermet, Kent, UK) followed by a 0.3 μm alumina−water slurry (Buehler) on a polishing cloth (Microcloth, Buehler). Periodic inspection of the electrodes using optical microscopy was performed to ensure that the disk had not recessed into the glass surface. The electrode diameters were calibrated electrochemically by analyzing the steady-state voltammetry of a 2 mM solution of ferrocene in acetonitrile containing 0.1 M TBAP, using a diffusion coefficient taken from the literature.[19]

The electrodes were housed in a glass cell designed for investigating microsamples of ionic liquids under a controlled atmosphere, a cross section of which is shown in Figure 1. The working electrode was modified with a section of a disposable micropipet tip to create a small cavity above the disk into which a drop (~10 μL) of ionic liquid was placed. The electrochemical cell was contained within a temperature-controlled box, constructed in house (see Figure 2) which doubled as a Faraday cage. The walls of the cage consisted of aluminum sheets separated by insulating Supawool 607 (RS Components Ltd., Northants, UK). Heat was supplied from a process heater mat (RS Components) located at the base of the cage and dispersed throughout it by a fan on the rear wall. The internal temperature

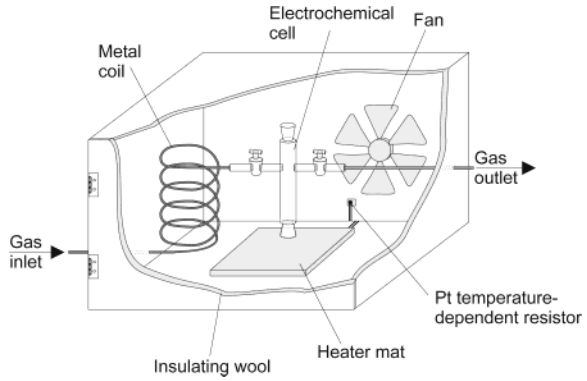

Figure 2. Schematic diagram of the temperature-controlled box.

was monitored by a platinum resistance thermometer (nominal resistance 100 Ω at room temperature) linked to a commercially available temperature controller (CAL 3200, CAL Controls Ltd., Herts., UK) situated outside the cage. Gas mixtures were introduced through a coiled metal pipe inside the box to allow the gas time to reach the appropriate temperature, prior to it entering the electrochemical cell. The gas then exited the box via an exhaust. Mixtures of oxygen and argon were generated using a Wösthoff triple gas mixing pump (Bochum, Germany), accurate to ±1%. Nitrogen was connected as the third gas (redundant for the purposes the work reported here) to ensure correct operation of the pump. All experiments were carried out at 35 ± 1 °C.

Theory

Analysis of Chronoamperometric Transients. Simultaneous determination of both the diffusion coefficient, *D*, and initial concentration, *c*, of oxygen was achieved through analysis of chronoamperometric measurements conducted at the disk electrodes. The time-dependent current response, *I*, resulting from the diffusion-controlled reduction of oxygen following a potential step at a disk electrode is given by the following expression.

$$I = -4nFDcr_d f(\tau) \tag{3}$$

where

$$f(\tau) = 0.7854 + 0.8863\tau^{-1/2} + 0.2146e^{-0.7823\tau^{-1/2}} \tag{4}$$

and

$$\tau = \frac{4Dt}{r_d^2} \tag{5}$$

Here, *n* represents the number of electrons transferred, *F* is the Faraday constant, r_d the radius of the disk electrode, and *t* the time. Although an approximation, this single expression, empirically derived by Shoup and Szabo,[20] is sufficient to describe the current response to within an accuracy of 0.6% over all τ. In the limit of low τ, eq 3 simplifies to the Cottrell equation, with an $I \propto cD^{1/2}$ dependence, whereas at high τ, a steady-state current is attained and $I \propto cD$. Accordingly, the fitting of experimental data to eq 3 recorded over a time incorporating both these regimes allows deconvolution of the parameters *D* and *c* and hence their simultaneous determination. Fitting was achieved using the nonlinear curve fitting function available in ORIGIN 6.0 (Microcal Software Inc.). After entering a value of r_d, the software was instructed to iterate through various values of *D* and *c* until the fit to the experimental data had been optimized.

Simulation of Cyclic Voltammetry. The mathematical model used to simulate the one-electron reduction of oxygen to superoxide at a disk electrode and its subsequent reoxidation back to O_2 was identical to the one implemented in an earlier publication which contains a full detailed description of the simulation procedure.[12] Briefly, the pertinent time-dependent mass transport equations and boundary conditions were re-expressed using a coordinate transformation developed by Amatore and Fosset[21] and then solved numerically in two dimensions using the alternating direction implicit (ADI) method.[22,23] The current−voltage response was then calculated from the resulting concentration profiles. As in the previous study, a spatial grid size of 700 × 700 points ($N\theta \times N\Gamma$, where θ and Γ are the transformed grid coordinates) was employed to ensure accurate simulation of both the forward and reverse waves given the expected disparity in the diffusion coefficients of oxygen and superoxide, respectively.[12] After inputting the disk radius and the values of *D* and *c* determined from the chronoamperometric analysis, the fit between the simulated and experimental voltammetry was optimized manually by varying the diffusion coefficient of superoxide, the formal electrode potential, E_f^0, the standard electrochemical rate constant, k_0, and the transfer coefficient, α.

In the case of oxygen reduction in the tetraalkylphosphonium-based RTILs, an alternative model was developed, full details of which are provided in the Appendix. The computer programs implementing the ADI method for each mathematical model were written in Borland Delphi 6 Professional Edition and executed on a PC based on an Intel Pentium 4, 2 GHz processor with 1 GB of RAM.

Results and Discussion

Reduction of Oxygen in the Quaternary Ammonium RTILs. To remove atmospheric oxygen and water vapor initially present in the ionic liquids, the cell was purged with pure argon prior to the commencement of any controlled addition of oxygen. The level of these impurities was monitored by running background cyclic voltammograms, and 1 h of purging was found to be more than sufficient to obtain a constant response. While the amount of water remaining after this 1 h preparatory stage was never explicitly measured, it was felt that owing to the subsequent observation of reversible oxygen reduction voltammetry (vide infra) the cell was thereafter operating under essentially anhydrous conditions. Upon addition of controlled amounts of oxygen to the cell, the time taken for equilibration between the gaseous and dissolved O_2 was determined by recording voltammograms periodically until the reduction wave reached a maximum. The time taken to attain equilibrium was dependent on the volume of ionic liquid placed in the cell; with larger volumes the gas has further to diffuse from the surface to the electrode tip. The amount of RTIL used was optimized at 10 μL, whereupon a delay of 20 min between altering the oxygen level and making electrochemical measurements ensured that full equilibration had occurred. The circuits regulating the temperature were activated at the beginning of the 1 h purge with pure argon so that the cell had ample time to reach this selected temperature prior to the introduction of oxygen. These procedures were adopted for the collection of all the data reported below.

Figure 3 displays cyclic voltammograms recorded for the reduction of oxygen (100 v/v%) in $[N_{6222}][N(Tf)_2]$ at each of the three electrode materials: Au, Pt, and GC. In accordance

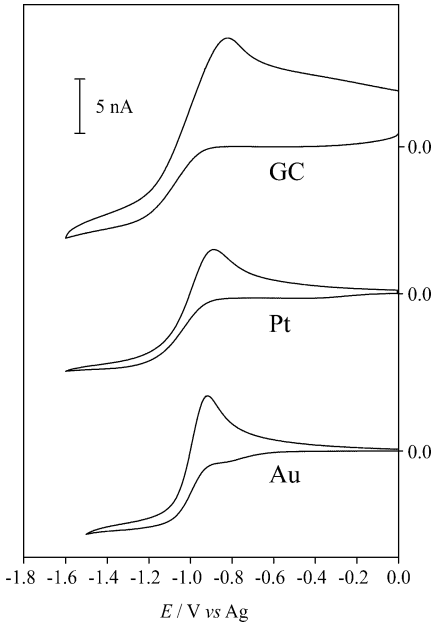

Figure 3. Cyclic voltammograms showing the reduction of oxygen in $[N_{6222}][N(Tf)_2]$ at Au, Pt, and GC disk electrodes, nominal radii 10 μm (Au, Pt) and 11 μm (GC), at a scan rate of 0.5 V s^{-1} and a temperature of 308 K.

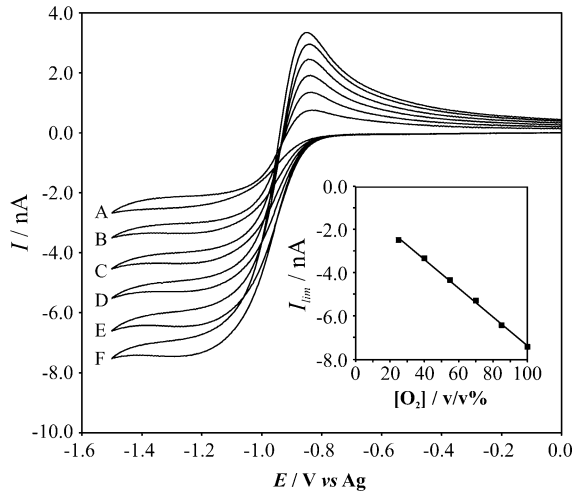

Figure 4. Cyclic voltammograms showing the reduction of (A) 25, (B) 40, (C) 55, (D) 70, (E) 85, and (F) 100 v/v% oxygen in $[Py_{14}][N(Tf)_2]$ at a 10 μm Au disk electrode, $v = 0.5$ V s^{-1}, $T = 308$ K. Inset shows the variation of limiting current with the proportion of oxygen in the gas phase ($R^2 = 0.9983$).

with the previous findings in this ionic liquid (at a Au electrode only),[12] distinctively asymmetric voltammetry is observed corresponding to the electrochemically reversible one-electron reduction of oxygen to give stable superoxide, which is subsequently reoxidized (eq 1). At the metal electrodes, a small prewave is apparent just prior to the onset of oxygen reduction. This is attributed to the presence of an unknown trace impurity in the ionic liquid, which could not be removed by any amount of purging with argon or exposure to vacuum conditions. By using 25 v/v% as a lower bound for the various oxygen concentrations introduced to the cell, however, the influence of this small signal on the overall voltammetry remained minimal. The reduction of oxygen in the second quaternary ammonium RTIL under study, $[Py_{14}][N(Tf)_2]$, followed the same pattern, as shown at a Au electrode in Figure 4 which exemplifies the typical voltammetric response of these systems to gradual exposure to increasing oxygen concentrations (25−100 v/v% in 15% increments). In all cases, the trend in limiting current for the forward process with concentration of oxygen added showed an excellent linearity.

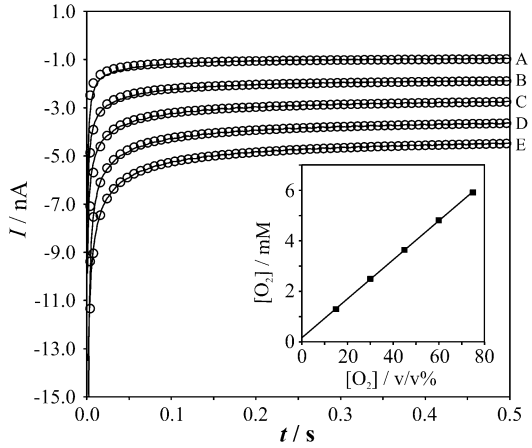

Figure 5. Experimental (—) and fitted theoretical (○) chronoamperometric transients for the reduction of (A) 15, (B) 30, (C) 45, (D) 60, and (E) 75 v/v% oxygen in $[N_{6222}][N(Tf)_2]$ at a 10 μm Au disk electrode, $T = 308$ K. Inset shows the variation of oxygen concentration in solution (deduced from the transients) with the proportion of oxygen in the gas phase ($R^2 = 0.9994$). Fitting parameters are listed in Table 1.

As outlined in the theoretical section, a chronoamperometric method was applied to deduce the concentration, c, and diffusion coefficient, $D(O_2)$, of the electroactive species in the ionic liquids. To ensure that the two-electrode system was initially at equilibrium, the potential was held at a point corresponding to the passage of no Faradaic current for a period of 300 s before being instantaneously stepped to a potential in the plateau region of the reductive wave. Transients were recorded at each of the six oxygen concentrations shown in Figure 4. To eliminate the influence of background currents (including those attributed to the low level impurity identified above), the transient for the lowest concentration, 25 v/v%, was subtracted from all the others. The corrected data were then analyzed according to the Shoup and Szabo expression[20] to yield unique values for the parameters c and $D(O_2)$ in each ionic liquid. A comparison of the experimental and fitted transients is shown in Figure 5 for the oxygen/$[N_{6222}][N(Tf)_2]$ system at a Au electrode. The fits are very close and the concentrations deduced directly proportional to the fraction of oxygen introduced to the cell. These data are typical of the results seen at the Au and Pt electrodes in both RTILs. At the GC electrode, however, the transients recorded were of lower quality and analysis by this means was unsuccessful. This is believed to be related to the rather large background current obtained at this electrode, which, as can be seen in Figure 3, is much larger than those present at the two metal electrodes and is beginning to swamp the signal of interest even when a pure oxygen atmosphere is used. Nevertheless, the data from two separate runs at each of the other two electrodes were averaged to give the final results, reported in Table 1. Encouragingly, these values are of the same order as equivalent data reported for oxygen in other ionic liquids.[10,12,24] The only direct comparison possible is with the earlier work on $[N_{6222}][N(Tf)_2]$ in which a concentration of 11.6 mM and diffusion coefficient of 1.5×10^{-10} m^2 s^{-1} were obtained at 293 K.[12] These results compare well with those from the current investigation, and the discrepancy can be rationalized by considering the variation in temperature. A temperature increase would be expected to provoke an increase in the diffusion rate (owing to a decrease in the solvent viscosity) and at the same time a reduction in solubility of any gaseous solute, just as the

TABLE 1: Saturated Concentration Values and Diffusion Coefficients for Oxygen in Room Temperature Ionic Liquid Solvents at Standard Pressure and 308 K[a]

	$[O_2]$ /mM	$D(O_2)$ /10^{-10} m^2 s^{-1}
$[N_{6222}][N(Tf)_2]$	8.9 ± 0.8	3.2 ± 0.3
$[Py_{14}][N(Tf)_2]$	6.1 ± 0.8	5.2 ± 0.4
$[P_{14.666}][N(Tf)_2]$	6.0 ± 0.5	7.5 ± 0.6
$[P_{14.666}][FAP]$	7.8 ± 1.5	6.1 ± 1.1

[a] Values are deduced from chronoamperometric measurements assuming in each case a simple one-electron transfer process.

TABLE 2: Electrochemical Parameters for the Reversible One-Electron Reduction of Oxygen in Two Quaternary Ammonium Room Temperature Ionic Liquids at 308 K

	$D(O_2^{-\bullet})$ /10^{-11} m^2 s^{-1}	E_f^0 /V vs Ag	k_0 /10^{-3} cm s^{-1}	α
$[N_{6222}][N(Tf)_2]$				
Au	1.45	−0.89	5.0	0.35
Pt	1.55	−0.91	3.0	0.33
$[Py_{14}][N(Tf)_2]$				
Au	3.35	−0.87	3.5	0.38
Pt	3.50	−0.86	0.8	0.35

data shows. Of the two quaternary ammonium RTILs studied, oxygen diffusion was more rapid in the pyrrolidinium salt, and this is again in accordance with its lower viscosity compared to that of $[N_{6222}][N(Tf)_2]$ (95 mPa s versus 220 mPa s at 293 K).[17,25]

To determine the remaining parameters for the electrochemical couple, experimental voltammograms were compared with computer simulations, starting with the now known values for c and $D(O_2)$, and varying $D(O_2^{-\bullet})$, E_f^0, k_0, and α in order to reproduce the observed voltammetry as closely as possible. A good fit was achieved for each system, as displayed in Figure 6, and the optimal parameters are listed in Table 2. Several points concerning these results merit some comment. The first thing to notice is that the values of $D(O_2^{-\bullet})$ and E_f^0 obtained for the same ionic liquid at the Au and Pt electrodes, respectively, are very similar. This bodes well for the accuracy of the simulations, since both these properties of the system should be independent of the electrode material. In both ionic liquids, the heterogeneous rate constant is lower on Pt than Au and the electron transfer coefficients are significantly below 0.5. This behavior is analogous to that seen for reduction of oxygen in traditional organic solvents where low transfer coefficients at metal electrodes and especially sluggish kinetics at platinum electrodes have previously been reported.[2,4,26] Finally, regarding the superoxide diffusion coefficients, they are confirmed as being over an order of magnitude lower than those of oxygen in the same media. Presumably, this results from the difference

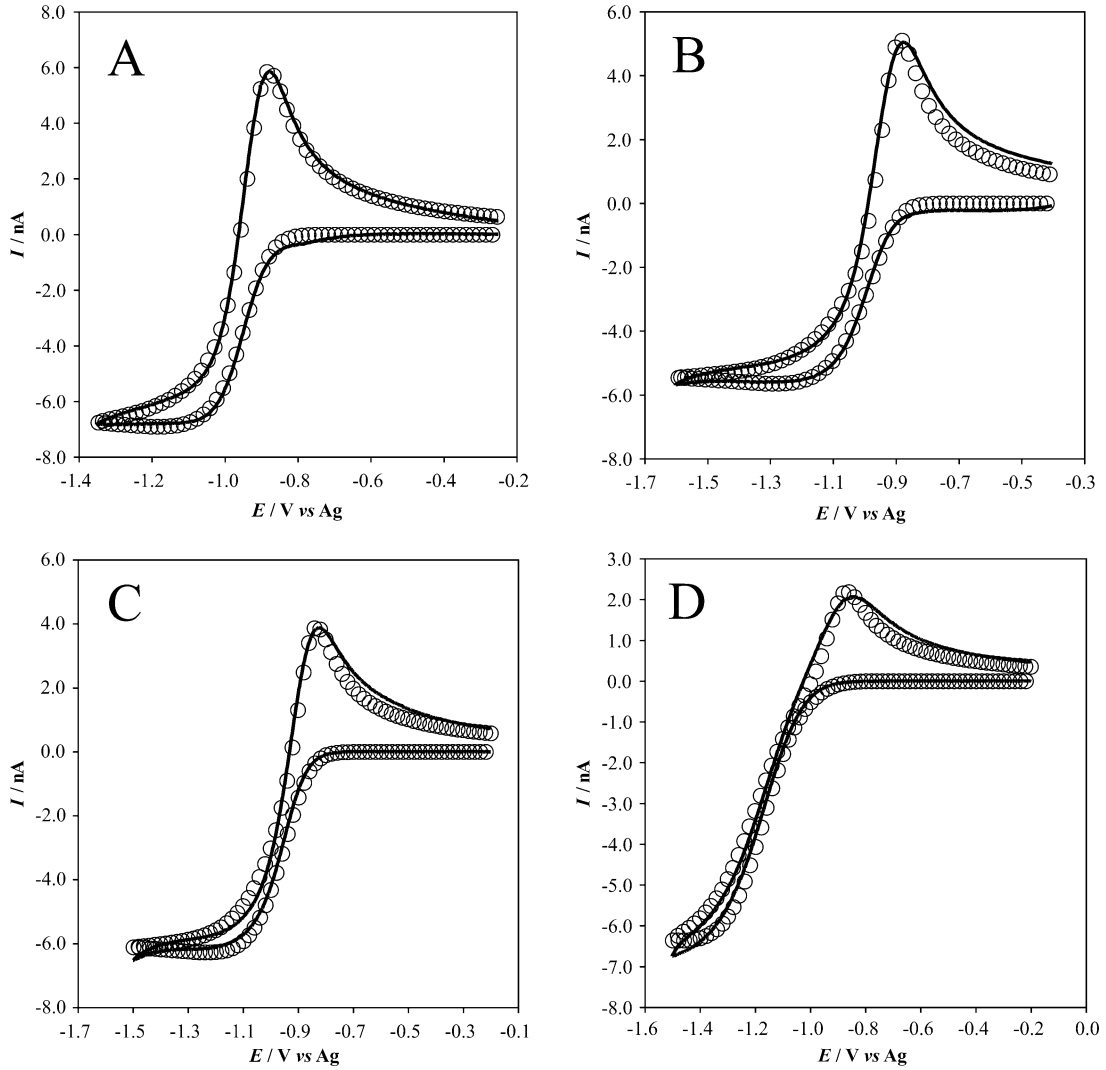

Figure 6. Comparison of experimental (—) and simulated (○) cyclic voltammograms for the reduction of oxygen in RTILs containing quaternary ammonium cations at 10 μm Au and Pt disk electrodes, $\upsilon = 1.0$ V s^{-1}. (A) Au/$[N_{6222}][N(Tf)_2]$, (B) Au/$[Py_{14}][N(Tf)_2]$, (C) Pt/$N_{6222}][N(Tf)_2]$, (D) Pt/$[Py_{14}][N(Tf)_2]$. Simulation parameters are listed in Table 2.

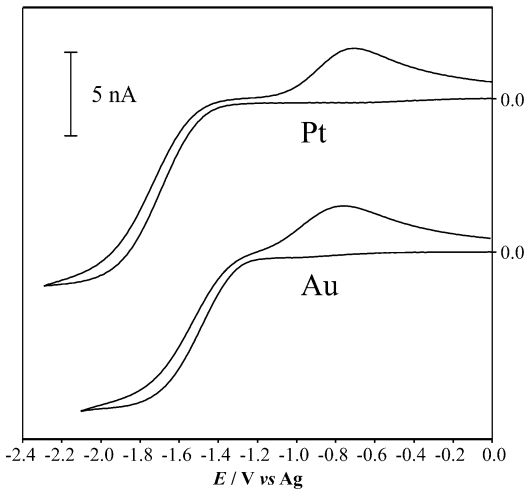

Figure 7. Cyclic voltammograms showing the reduction of oxygen in $[P_{14.666}][FAP]$ at 10 μm Au and Pt disk electrodes, $\upsilon = 0.5$ V s^{-1}, $T =$ 308 K.

in the strength of the Coulombic forces between these highly ionic solvents and the neutral oxygen molecule and superoxide radical anion, respectively. In any case, the combination of this disparity in the diffusion rates of the reduced and oxidized species with a disk electrode of appropriate radius explains the observed asymmetry in the voltammetry of this system. Over the same experimental time scale, the faster diffusion rate of oxygen causes a spherical diffusion layer to develop at the electrode surface leading to steady-state behavior, whereas supply of the more slowly moving superoxide is always dominated by planar diffusion normal to the surface, resulting in a peak-shaped transient reverse wave.

Reduction of Oxygen in the Quaternary Phosphonium RTILs. Attention now turns to the voltammetry of oxygen in the two ionic liquids containing the quaternary phosphonium cation, $[P_{14.666}]$. Figure 7 shows cyclic voltammograms for the reduction of 100 v/v% O_2 in the RTIL $[P_{14.666}][FAP]$ at Au and Pt electrodes. While a steady-state forward wave similar to that seen for the quaternary ammonium ionic liquids is again observed, the oxidation peaks are broader and further removed from the initial reductive wave, in the case of the Pt electrode markedly so. The limiting currents derived from the forward wave again varied linearly with the proportion of oxygen gas introduced, and a chronoamperometric analysis equivalent to the one described in the previous section (i.e., assuming that the process involved was the one-electron reduction of oxygen) was performed to attempt to deduce the O_2 concentration and diffusion coefficient. A good correlation was again achieved, and the derived values for c and $D(O_2)$ are given in Table 1. It is interesting to note that the oxygen solubility does not vary significantly between the $[N(Tf)_2]$ and [FAP] anions despite the large increase in the fluorine content. With the use of these values, a simulation of the observed voltammetry was attempted using the above model for a simple reversible single electron transfer. However, while the reductive wave could be quite successfully modeled, it was impossible to achieve at the same time a satisfactory fit of the back peak. This simple mechanism was therefore deemed inconsistent with the observed results. The current−voltage profile was in fact much more reminiscent of the voltammetry of oxygen in an aprotic solvent following the addition of a proton source (vide supra). Since the only species present are oxygen and the solvent itself, the most likely proton source is the quaternary phosphonium cation.

On this basis, an alternative mechanism is proposed involving α-proton abstraction from $[P_{14.666}]$ by superoxide.

$$O_2^{-\bullet} + R_3\overset{+}{P}CH_2R' \rightarrow HO_2^{\bullet} + R_3P{=}CHR' \qquad (6)$$

This is by no means unfeasible considering that the reaction of phosphonium ions with strong bases is well established, most notably in the Wittig alkene synthesis, in which the initial step is deprotonation to give a phosphorus ylide.[27] Furthermore, this would explain why a similar process is not observed with the quaternary ammonium salts, whose chemistry bears little in common with their phosphonium analogues; unlike nitrogen, phosphorus is able to adopt a pentacovalent state and is much better at stabilizing a negative charge at an α-C.[27] One possible fate for the protonated form of superoxide is to undergo disproportionation to give hydrogen peroxide and regenerate oxygen.

$$2HO_2^{\bullet} \rightarrow H_2O_2 + O_2 \qquad (7)$$

In this way, the number of electrons for the forward process may vary between one and two, depending on the rate of reactions 6 and 7 relative to the experimental time scale. Having recognized this, it must be appreciated that the diffusion coefficients given for oxygen in Table 2 for the two phosphonium-derived ionic liquids should be considered as upper bounds, and their true values may be somewhat lower, depending on the exact number of electrons transferred. The peak observed on the reverse scan may result from oxidation of the phosphorus ylide or, conceivably, either the perhydroxyl radical itself or some oxygen-derived species produced in follow up reactions. On repetitive cycling, the voltammetry showed little change and the emergence of no new peaks, implying that the oxidation is irreversible. In experiments with conventional organic solvents, the equivalent peak has been attributed to oxidation of the conjugate base from the Brønsted acid added as a proton source (here, the phosphorus ylide).[2,6] The electrochemical properties of phosphorus ylides have not been widely studied, but a single report on several such compounds in acetonitrile suggests that they are susceptible to being oxidized irreversibly to give highly reactive radical anions.[28]

To corroborate the proposed mechanism, the voltammetry of oxygen in $[N_{6222}][N(Tf)_2]$ was reinvestigated upon addition of a proton source. A 25 mM solution of catechol in $[N_{6222}][N(Tf)_2]$ was prepared using a solvent evaporation-based procedure (details of which are described elsewhere[17]). Figure 8 shows the reduction of 100 v/v% oxygen at a Pt electrode in both the pure ionic liquid and the acidified solution. As catechol is a stronger acid than the $[P_{14.666}]$ ion, a shoulder due to the reduction of protons may be observed on the forward wave in the latter voltammogram. Nevertheless, the effect on the back peak is clear; the sharp peak at −0.89 V versus Ag is replaced by a broader signal displaced by about 0.8 V from the reduction wave, just as was observed in the phosphonium-based ionic liquids. This would suggest that the electroactive product responsible for the back peak is common to both systems and is therefore an oxygen-derived species.

A full theoretical treatment of the voltammetry of oxygen in quaternary phosphonium RTILs is not straightforward given the number of species involved and the uncertainty in the exact nature of the follow up chemistry after the proton abstraction step. By applying a general $\bar{E}C\bar{E}$ model, however, it is possible to characterize the heterogeneous steps of the mechanism. Applying this model, the reaction is considered to proceed via

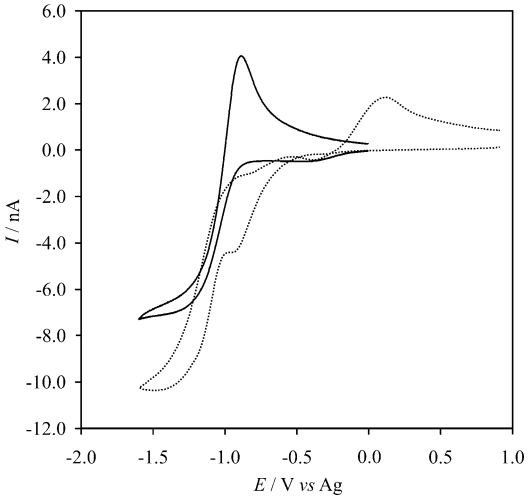

Figure 8. Cyclic voltammograms showing the reduction of 100 v/v% oxygen in $[N_{6222}][N(Tf)_2]$ at a 10 μm Pt disk electrode in the presence (···) and absence (—) of 25 mM catechol, $\upsilon = 0.5$ V s^{-1}, $T = 308$ K.

TABLE 3: Electrochemical Parameters for the Reduction of Oxygen via an ECE Mechanism in Two Quaternary Phosphonium Room Temperature Ionic Liquids at 308 K[a]

	$E_f^{0'}$ /V vs Ag	k_0' /10^{-3} cm s^{-1}	α′	D(X) /10^{-11} m^2 s^{-1}	α″
$[P_{14.666}][N(Tf)_2]$					
Au	−0.75	1.77	0.38	0.59	0.63
Pt	−0.75	0.14	0.31	0.41	0.69
$[P_{14.666}][FAP]$					
Au	−1.10	0.11	0.32	0.31	0.75
Pt	−1.10	0.05	0.25	0.37	0.75

[a] The superscripts ′ and ″ refer to the first and second heterogeneous steps, respectively, and X represents the species that undergoes the second electron transfer (see text).

an initial one-electron heterogeneous electron transfer followed by a diffusion-controlled, first-order, irreversible chemical step to yield another electroactive species, which then undergoes the second one-electron heterogeneous electron transfer (in the opposite direction to the first), as shown in the following scheme

$$O_2 + e^- \rightleftharpoons O_2^{-\bullet} \qquad \vec{E}$$

$$O_2^{-\bullet} \rightarrow \rightarrow X(Red) \qquad C$$

$$X(Red) \rightarrow X(Ox) + e^- \qquad \overleftarrow{E}$$

where X(Red) and X(Ox) represent the reduced and oxidized forms of the electroactive species responsible for the oxidation peak on the reverse scan. The full details of this simulation are provided in the Appendix. Fitting to the experimental voltammetry was achieved by applying the values of c and $D(O_2)$ calculated from the chronoamperometric measurements and then varying the remaining parameters systematically. The optimized values are shown in Table 3, and examples of the fits are displayed in Figure 9.

Conclusions

Four room temperature ionic liquids comprised of group 15-centered cations and anions have been employed as electrolytes in which to study the electrochemical reduction of dioxygen. In the quaternary ammonium RTILs $[N_{6222}][N(Tf)_2]$ and $[Py_{14}][N(Tf)_2]$ the reduction was found to proceed reversibly (in the chemical sense) via the loss of one-electron to yield the superoxide radical which was stable in these media. Voltammetric and chronoamperometric data were analyzed against the appropriate theoretical models to extract a full set of thermodynamic and kinetic parameters for this electrochemical couple. While the diffusion coefficients of oxygen and superoxide are found to be 10−100 times smaller than in simple organic solvents, in accordance with previous findings (and a consequence of the higher viscosity of RTILs), the results indicate that the process is otherwise not significantly altered; trends in the behavior of the heterogeneous rate constant and electron transfer coefficient at different electrode materials were preserved. In contrast, the voltammetry of oxygen in the quaternary phosphonium RTILs $[P_{14.666}][N(Tf)_2]$ and $[P_{14.666}][FAP]$ was found to proceed by a different mechanism. The presence of the weakly acidic $[P_{14.666}]$ renders superoxide unstable in these solvents with respect to the formation of a perhydroxyl radical and phosphorus ylide and, through follow up homogeneous reactions, the partial regeneration of O_2. Reduction of oxygen is therefore irreversible, involving the transfer of between one and two electrons. This behavior represents an intermediate case between the one-election reduction of oxygen in aprotic organic solvents and the two-electron process observed in aqueous solution where the protonation and subsequent reactions of the superoxide are extremely rapid. Although a complete characterization of this reaction scheme in the RTILs will require

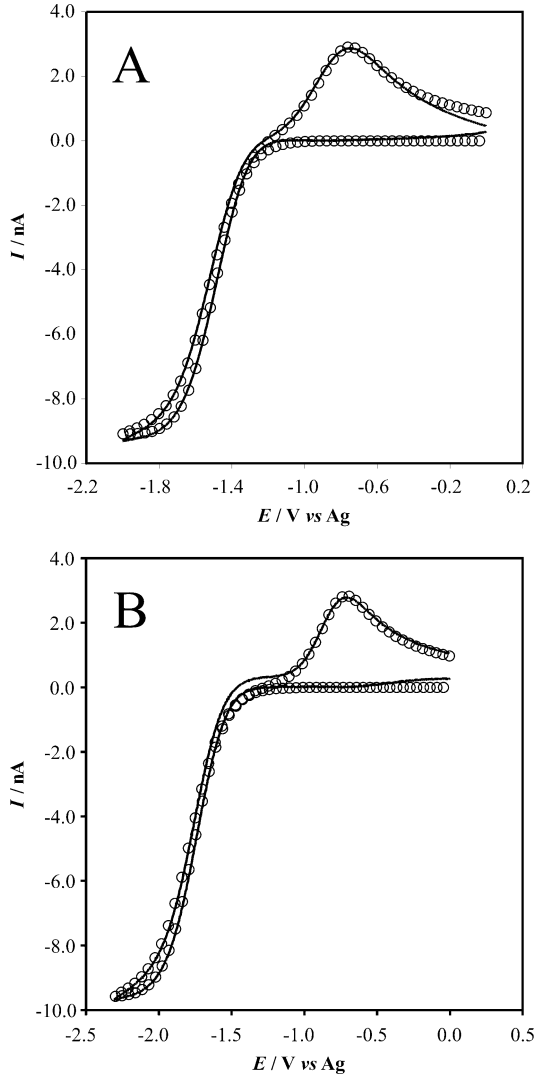

Figure 9. Comparison of experimental (—) and simulated (○) cyclic voltammograms for the reduction of oxygen in $[P_{14.666}][FAP]$ at 10 μm (A) Au and (B) Pt disk electrodes, $\upsilon = 0.5$ V s^{-1}. Simulation parameters are listed in Table 3.

further experimentation, a partial parametrization of the heterogeneous steps was achieved through the application of a generalized $\vec{E}C\vec{E}$ mechanism.

Acknowledgment. R.G.E. thanks the EPSRC for funding via a project studentship, and O.V.K. acknowledges the Clarendon Fund for partial support. The authors are grateful to Merck KGaA for supplying the $[P_{14.666}][FAP]$ ionic liquid, Professor Clive Hahn for the loan of the gas mixing pump, and Michael Hyde for preparing some of the illustrations.

Appendix

Simulating the $\vec{E}C\vec{E}$ Mechanism for Oxygen Reduction in Quaternary Phosphonium Ionic Liquids. The reaction mechanism described for the reduction of oxygen in the quaternary phosphonium ionic liquids may be written in symbolic form as

$$\begin{aligned} A + e^- &\rightleftharpoons B \\ B &\underset{k^-}{\overset{k^+}{\rightleftharpoons}} C \\ C &\rightleftharpoons D + e^- \end{aligned} \tag{8}$$

where A is oxygen, B is superoxide, k^+ is the rate constant of the forward homogeneous reaction, and k^- is the rate constant of the reverse reaction. As explained above, the identity of species C is not known with absolute certainty. It is either some oxygen-derived species or the phosphorus ylide, but in the absence of further experimentation, neither possibility can be entirely ruled out. In any case, species D is then the product of its oxidation.

Reaction scheme 8 is considered as taking place at a disk electrode under cyclic voltammetric conditions. The mass transport equations describing the concentration distribution of the species in the solution are

$$\begin{aligned} \frac{\partial[A]}{\partial t} &= D_A\left(\frac{\partial^2[A]}{\partial r^2} + \frac{1}{r}\frac{\partial[A]}{\partial r} + \frac{\partial^2[A]}{\partial z^2}\right) \\ \frac{\partial[B]}{\partial t} &= D_B\left(\frac{\partial^2[B]}{\partial r^2} + \frac{1}{r}\frac{\partial[B]}{\partial r} + \frac{\partial^2[B]}{\partial z^2}\right) - k^+[B] + k^-[C] \\ \frac{\partial[C]}{\partial t} &= D_C\left(\frac{\partial^2[C]}{\partial r^2} + \frac{1}{r}\frac{\partial[C]}{\partial r} + \frac{\partial^2[C]}{\partial z^2}\right) + k^+[B] - k^-[C] \end{aligned} \tag{9}$$

where D_A is the diffusion coefficient of species A, etc., r and z are cylindrical coordinates, and t is time. Initially the solution contains only species A at a bulk concentration $[A]_{bulk}$ which leads to the following initial conditions:

$$\begin{aligned} [A](r,z,0) &= [A]_{bulk} \\ [B](r,z,0) &= [C](r,z,0) = 0 \end{aligned} \tag{10}$$

The system of partial differential equations (eq 9) must be completed with the following boundary conditions given by the Butler−Volmer theory at the electrode surface, no flux conditions at the insulator and symmetry axis, and bulk concentration far away from the electrode:

$$\begin{aligned} z = 0,\ 0 \le r \le r_d \quad & D_A\left.\frac{\partial[A]}{\partial z}\right|_{z=0} = (k'_f[A] - k'_b[B])_{z=0}; \\ & D_B\left.\frac{\partial[B]}{\partial z}\right|_{z=0} = -D_A\left.\frac{\partial[A]}{\partial z}\right|_{z=0} \\ & D_C\left.\frac{\partial[C]}{\partial z}\right|_{z=0} = k''_f[C]_{z=0} \\ z = 0,\ r > r_d \quad & \left.\frac{\partial[A]}{\partial z}\right|_{z=0} = \left.\frac{\partial[B]}{\partial z}\right|_{z=0} = \left.\frac{\partial[C]}{\partial z}\right|_{z=0} = 0 \\ \text{all } z,\ r = 0 \quad & \left.\frac{\partial[A]}{\partial r}\right|_{r=0} = \left.\frac{\partial[B]}{\partial r}\right|_{r=0} = \left.\frac{\partial[C]}{\partial r}\right|_{r=0} = 0 \\ z,\ r \to \infty \quad & [A] \to [A]_{bulk};\quad [B] \to 0;\quad [C] \to 0 \end{aligned} \tag{11}$$

where the forward (marked with a subscript f) and backward (marked with a subscript b) heterogeneous rate constants are given by

$$\begin{aligned} k'_f &= k'_0 \exp\left(\frac{-\alpha' F}{RT}(E - E_f^{0'})\right) \\ k'_b &= k'_0 \exp\left(\frac{(1-\alpha')F}{RT}(E - E_f^{0'})\right) \\ k''_f &= k''_0 \exp\left(\frac{(1-\alpha'')F}{RT}(E - E_f^{0})\right) \end{aligned} \tag{12}$$

where k'_0 and k''_0 are the standard heterogeneous rate constants, α' and α'' are transfer coefficients, and $E_f^{0'}$ and $E_f^{0''}$ are the formal potentials of the redox couples A/B and C/D in the first and the third steps in reaction scheme 8, respectively.

The boundary condition for the species C at the electrode surface given in eq 10 is used here instead of the full Butler−Volmer expression because of high irreversibility of the third reaction in the mechanism 8 (vide supra). This makes the effect of the reduction of the species D back to C on the current negligible, and thus the corresponding term $(-k''_b[D])$ has been dropped from the boundary condition for species C. Consequently the mass transport equation for the species D has not been considered. Moreover, it follows that in this case it is impossible to determine the values of the standard heterogeneous rate constant k''_0 and the formal potential $E_f^{0''}$ independently. Indeed, the boundary condition for C depends only on k''_f but not on k''_b. The former may be represented in the following form

$$k''_f = k''_0 \exp\left(\frac{(\alpha'' - 1)FE_f^{0''}}{RT}\right)\exp\left(\frac{(1-\alpha'')FE}{RT}\right) = k_0(\alpha'')\exp\left(\frac{(1-\alpha'')FE}{RT}\right) \tag{13}$$

Obviously, there are an infinite number of pairs k''_0, $E_f^{0''}$ corresponding to the same value of $k_0(\alpha'')$. Therefore it is impossible to find a unique solution for these two parameters.

The current flowing at the surface of a disk electrode is given by the following integral:

$$i = 2\pi F D_A \int_0^{r_d}\left(\frac{\partial[C]}{\partial z} - \frac{\partial[A]}{\partial z}\right)_{z=0} r\,dr \tag{14}$$

The mathematical model 9−11 was normalized with subsequent application of the coordinate transformation developed by Amatore and Fosset for microdisk electrode geometry.[21] The resulting equations were then discretised according to the ADI method.[22,23] The banded systems of linear algebraic equations produced by the implicit ADI method were solved using the generalized Thomas algorithm.[29]

The error analysis similar to that described previously[12,30,31] was applied to determine the simulation grid size necessary to achieve the desired accuracy for the expected ranges of the parameter variation. This resulted in a spatial grid size of 350 $\times$ 350 ($N\theta \times N\Gamma$) required to achieve the accuracy of not worse than 1%. Such a high number of mesh nodes in space is necessitated by the fact that the diffusion coefficients of the reacting species may differ by more than 2 orders of magnitude.[12] A typical computational time for simulation of a cyclic voltammogram within 1% accuracy was approximately 20 min. However, significantly smaller grids can be used for the initial fitting of the experimental voltammograms with less computational effort and the final verification performed at a 300 $\times$ 300 grid.

The convergence error appeared to be virtually independent of the discretisation in time. Therefore the number of points in time was kept constant at 2000 to ensure the smoothness of the simulated voltammograms.

References and Notes

(1) Sawyer, D. T.; Sobkowiak, A.; Roberts, J. L. *Electrochemistry for Chemists*, 2nd ed.; Wiley-Interscience: New York, 1995; Chapter 9.
(2) Sawyer, D. T.; Chiericato, G., Jr.; Angelis, C. T.; Nanni, E. J., Jr.; Tsuchiya, T. *Anal. Chem.* **1982**, *54*, 1720.
(3) Wadhawan, J. D.; Welford, P. J.; McPeak, H. B.; Hahn, C. E. W.; Compton, R. G. *Sens. Actuators B* **2003**, *B88*, 40.
(4) Vasudevan, D.; Wendt, H. *J. Electroanal. Chem.* **1995**, *392*, 69.
(5) Cofre, P.; Sawyer, D. T. *Anal. Chem.* **1986**, *58*, 1057.
(6) Andrieux, C. P.; Hapiot, P.; Saveant, J. M. *J. Am. Chem. Soc.* **1987**, *109*, 3768.
(7) Buzzeo, M. C.; Evans, R. G.; Compton, R. G. *ChemPhysChem.*, in press.
(8) Carter, M. T.; Hussey, C. L.; Strubinger, S. K. D.; Osteryoung, R. A. *Inorg. Chem.* **1991**, *30*, 1149.
(9) Buzzeo, M. C.; Klymenko, O. V.; Wadhawan, J. D.; Hardacre, C.; Seddon, K. R.; Compton, R. G. *J. Phys. Chem. B* **2004**, *108*, 3947.
(10) AlNashef, I. M.; Leonard, M. L.; Kittle, M. C.; Matthews, M. A.; Weidner, J. W. *Electrochem. Solid-State Lett.* **2001**, *4*, D16.
(11) AlNashef, I. M.; Leonard, M. L.; Matthews, M. A.; Weidner, J. W. *Ind. Eng. Chem. Res.* **2002**, *41*, 4475.
(12) Buzzeo, M. C.; Klymenko, O. V.; Wadhawan, J. D.; Hardacre, C.; Seddon, K. R.; Compton, R. G. *J. Phys. Chem. A* **2003**, *107*, 8872.
(13) MacFarlane, D. R.; Meakin, P.; Sun, J.; Amini, N.; Forsyth, M. *J. Phys. Chem. B* **1999**, *103*, 4164.
(14) Xu, K.; Ding, M. S.; Jow, T. R. *J. Electrochem. Soc.* **2001**, *148*, A267.
(15) Sun, J.; Forsyth, M.; MacFarlane, D. R. *J. Phys. Chem. B* **1998**, *102*, 8858.
(16) McEwen, A. B.; Ngo, E. L.; LeCompte, K.; Goldman, J. L. *J. Electrochem. Soc.* **1999**, *146*, 1687.
(17) Evans, R. G.; Klymenko, O. V.; Hardacre, C.; Seddon, K. R.; Compton, R. G. *J. Electroanal. Chem.* **2003**, *556*, 179.
(18) Bonhôte, P.; Dias, A.-P.; Armand, M.; Papageorgiou, N.; Kalyanasundaram, K.; Grätzel, M. *Inorg. Chem.* **1996**, *35*, 1168.
(19) Coles, B. A.; Moorcroft, M. J.; Compton, R. G. *J. Electroanal. Chem.* **2001**, *513*, 87.
(20) Shoup, D.; Szabo, A. *J. Electroanal. Chem.* **1982**, *140*, 237.
(21) Amatore, C. A.; Fosset, B. *J. Electroanal. Chem.* **1992**, *328*, 21.
(22) Heinze, J. *J. Electroanal. Chem.* **1981**, *124*, 73.
(23) Svir, I. B.; Klymenko, O. V.; Compton, R. G. *Radiotekhnika* **2001**, *118*, 92.
(24) Anthony, J. L.; Maginn, E. J.; Brennecke, J. F. *J. Phys. Chem. B* **2002**, *106*, 7315.
(25) Pitner, W. R.; Hardacre, C. Unpublished results.
(26) Jain, P. S.; Lal, S. *Electrochim. Acta* **1982**, *27*, 759.
(27) Quin, L. D. *A Guide to Organophosphorus Chemistry*; Wiley: New York, 2000.
(28) Monastyrskaya, V. I.; Kalnin'sh, K. K.; Strunin, B. N.; Tsalieva, A. G. *Russ. J. Gen. Chem.* **1997**, *67*, 570.
(29) Eriksson, K.; Estep, D.; Hansbo, P.; Johnson, C. *Computational Differential Equations*; Cambridge University Press: Cambridge, 1996.
(30) Klymenko, O. V.; Giovanelli, D.; Lawrence, N. S.; Rees, N. V.; Jiang, L.; Jones, T. G. J.; Compton, R. G. *Electroanalysis* **2003**, *15*, 949.
(31) Rees, N. V.; Klymenko, O. V.; Compton, R. G.; Oyama, M. *J. Electroanal. Chem.* **2002**, *531*, 33.